

The logo of the Federal University of Paraná (UFPR) is visible as a watermark on the left side of the slide. It features a stylized flame above an open book with the Greek letters Alpha (Α) and Omega (Ω) on its pages, and a map of the state of Paraná below. The entire logo is rendered in a light gray color.

Photoproduction of Upsilon states in ultraperipheral collisions at the LHC ¹

Magno V T Machado
<magnus@ufprgs.br>

XLVII International Symposium on Multiparticle Dynamics (ISMD2017)
September 11 – 15, 2017. Tlaxcala City, Mexico.

¹In collaboration with MB Gay Ducati, F Kopp, S Martins [PRD94 (2016) 094023, PRD96(2017)054001]

- Introduction

- Ultrapерipheral Collisions (UPCs)
- The photon flux and the photoproduction cross section
- Exclusive photoproduction → Pomeron exchange

- Vector mesons production in pp and PbPb collisions

- Differential cross section calculation in the dipole formalism
- Vector mesons wave function
- Dipole cross section model

- Results for $V = (J/\psi, \psi', Y(1S) \text{ and } Y(2S, 3S))$ production

- Rapidity distribution of vector meson photoproduction
 - Proton-Proton collisions
 - Pb-Pb collisions

- Summary

Why to Investigate the Quarkonium Production?

Introduction

Cross Section Calculation

Results

Summary

- In pp collisions

- Heavy-quark mass acts as a long distance cut-off
 - pQCD down to low transverse momenta (p_T).

- Test for both perturbative and non-perturbative aspects of QCD calculations.

- In nuclear collisions

- Open and hidden heavy-flavour production constitutes a sensitive probe of the QGP.

- The in-medium dissociation probability of these states are expected to provide an estimate of the initial temperature reached in the collisions.

- The nuclear modification of the PDFs can also be studied using quarkonium photoproduction in ultra-peripheral nucleus–nucleus collisions.

Quarkonium Production Mechanisms

Introduction

Cross
Section
Calculation

Results

Summary

- Hadroproduction

- Colour Singlet Model (CSM).
 - heavy quark pair production with the same quantum numbers as the final-state meson
- Colour Octet Model (COM).
 - both colorless and colored states of the heavy quark pairs are considered.
 - the relative contribution of the states is parametrized
- Colour Evaporation Model.
 - cross section of a given quarkonium is proportional to the heavy quark pair cross section.
- NRQCD combines COM and CSM aspects.

Quarkonium Production Mechanisms

Introduction

Cross Section Calculation

Results

Summary

- Photoproduction

- Vector Meson Dominance.
- LO (NLO) perturbative QCD calculations.
- **Colour Dipole Model.**
 - Photoproduction cross section is factorized in photon-meson wave function and color dipole cross section.
 - Meson wavefunction describes dipole-meson transition.
 - Dipole cross section describes dipole-target interaction.

Photoproduction - Theoretical Motivation

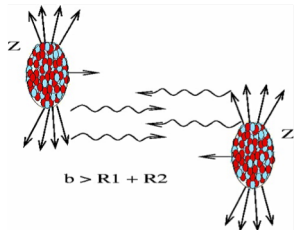
Introduction

Cross Section Calculation

Results

Summary

The photoproduction is dominant in ultra-peripheral scattering ($b_{\text{impact}} > 2R_A$).



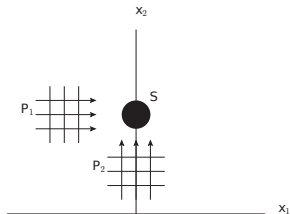
From Weizsäcker-Williams method, the UPC cross section for a given X final state can be given by

$$\sigma_X = \int d\omega \frac{dN(\omega)}{d\omega} \sigma_X^\gamma(\omega)$$

where,

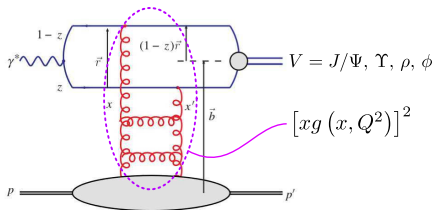
$\frac{dN(\omega)}{d\omega} \rightarrow$ Photon Flux

$\sigma_X^\gamma(\omega) \rightarrow$ Photoproduction Cross Section



Exclusive vector meson photoproduction

- $\gamma + p \rightarrow V + p \rightarrow$ has been investigated experimentally and theoretically as it allows to test perturbative Quantum Chromodynamics.
- The quarkonium masses ($\simeq 2m_c, 2m_b$), give a perturbative scale for the problem even at $Q^2 = 0$.
- The **exclusive** photoproduction of mesons in the high energy regime is a possibility to investigate the Pomeron exchange.



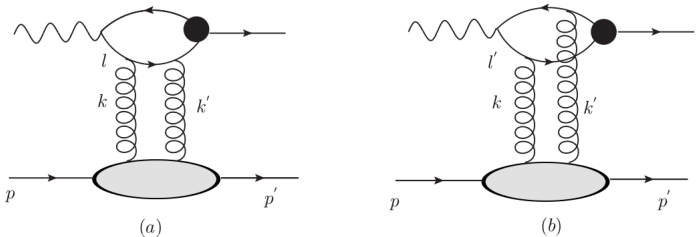
Pomeron \rightarrow two gluons (vacuum quantum numbers)

$x(x')$ \rightarrow gluon momentum fraction;

z \rightarrow quark momentum fraction;

Diffractive production of mesons at $t = 0$

- An important class of diffractive reactions where we can use a perturbative treatment is the exclusive vector meson production in DIS: $\gamma^* p \rightarrow V p$.
- Two gluons exchange diagrams that contribute to the amplitude of the vector meson leptonproduction are shown in the figure below:



In the color dipole formalism, the amplitude can be written as:

$$A \propto \Psi^\gamma \otimes \sigma^{q\bar{q}} \otimes \Psi^V, \quad (1)$$

Diffractive production of mesons at $t = 0$ in pQCD approach

Introduction

Cross
Section
Calculation

Results

Summary

Amplitude ²:

$$A_T(W^2, t = 0) = -4\pi^2 i \alpha_s W^2 \int \frac{dk^2}{k^4} \left(\frac{1}{l^2 - m_f^2} - \frac{1}{l'^2 - m_f^2} \right) f(x, k^2) e_c g_V M_V \quad (2)$$

$g_V^2 = 3\Gamma_{ee} M_V / 64\pi\alpha^2 \rightarrow$ specifies the $q\bar{q}$ coupling to the vector meson

$\Gamma_{ee} \rightarrow$ width decay $V \rightarrow e^+ e^-$

$e_c \rightarrow \frac{2}{3}$ for $\psi_{(1S),(2S)}$ and $\frac{1}{3}$ for $Y_{(1S),(2S)}$

$f(x, k^2) \rightarrow$ unintegrated gluons distribution.

$k, l(l') \rightarrow$ gluons transverse momentum and quark (antiquark) momentum

$m_f, m_V \rightarrow$ quark mass (m_c or m_b) and vector meson mass, respectively.

The complete differential cross section (T+L) in the $\ln \tilde{Q}^2$ dominant is:

$$\left. \frac{d\sigma^{\gamma^{(*)}p \rightarrow Vp}}{dt} \right|_{t=0} = \frac{16\Gamma_{e^+e^-}^V M_V^3 \pi^3}{3\alpha_{em}(Q^2 + M_V^2)^4} \left[\alpha_s(\tilde{Q}^2) xg(x, \tilde{Q}^2) \right]^2 \left(1 + \frac{Q^2}{M_V^2} \right)$$

$xg(x, \tilde{Q}^2) \rightarrow$ grows in small - $x \rightarrow$ undetermined

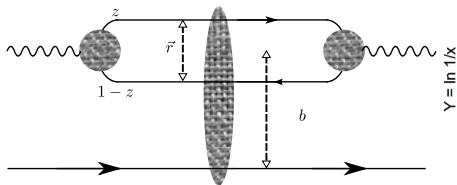
Dipole formalism \rightarrow can restrict $xg(x, \tilde{Q}^2) \rightarrow$ includes gluon saturation

²M. G. Ryskin, Z. Phys. C 57, 89, 1993

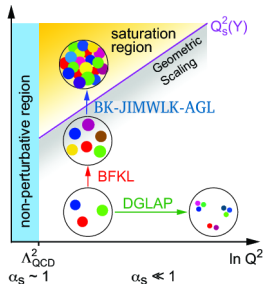
Dipole Formalism

- In the LHC energy domain virtual photons can be considered as color dipoles in the light cone representation³.

- The scattering process is characterized by the color dipole cross section representing their interaction with the target (includes the underlying QCD dynamics).



$r \rightarrow$ dipole separation.
 $z(1-z) \rightarrow$ quark(antiquark) momentum fraction.
 $b \rightarrow$ impact parameter.



³N. N. Nikolaev, B. G. Zakharov, Z. Phys. C 49, 607, 1991

Quarkonium production in pp collisions

Introduction

Cross
Section
Calculation

Results

Summary

The rapidity distribution for exclusive quarkonium photoproduction is given by

$$\frac{d\sigma}{dy}(pp \rightarrow p \otimes V \otimes p) = S_{\text{gap}}^2 \left[\omega \frac{dN_\gamma}{d\omega} \sigma(\gamma p \rightarrow V + p) + (y \rightarrow -y) \right]$$

Photon flux: ⁴

$$\frac{dN_\gamma(\omega)}{d\omega} = \frac{\alpha_{em}}{2\pi\omega} \left[1 + \left(1 - \frac{2\omega}{\sqrt{s}} \right)^2 \right] \times \left(\ln \xi - \frac{11}{6} + \frac{3}{\xi} - \frac{3}{2\xi^2} + \frac{1}{3\xi^3} \right) \quad (3)$$

$\omega \rightarrow$ photon energy

$S_{\text{gap}}^2 \sim 0.8$ for J/ψ ⁵ \rightarrow represents the absorptive corrections due to spectator interactions between the two hadrons - **Average**

⁴C. A. Bertulani, S. R. Klein and J. Nystrand, Ann. Rev. Nucl. Part. Sci. 55, 271, 2005

⁵W. Schafer and A. Szczurek, Phys. Rev. D 76, 094014, 2007

$$\sigma_{\gamma^* p \rightarrow V p}(X, Q^2) = \frac{1}{16\pi B_V} \left| \mathcal{A}(X, Q^2, \Delta = 0) \right|^2, \quad (4)$$

where the scattering amplitude is ⁶

$$\mathcal{A}(X, Q^2, \Delta) = \sum_{h, \bar{h}} \int dz d^2 r \Psi_{h, \bar{h}}^\gamma \mathcal{A}_{q\bar{q}}(X, r, \Delta) \Psi_{h, \bar{h}}^{V*}, \quad (5)$$

$B_V(W_{\gamma p}) = b_{el}^V + 2\alpha' \log\left(\frac{W_{\gamma p}}{W_0}\right)^2 \rightarrow$ diffractive slope parameter

$$\alpha' = 0.25 \text{ GeV}^{-2}$$

$$W_0 = 95 \text{ GeV}$$

$$b_{el}^{\Psi(1S)} = 4.99 \pm 0.41 \text{ GeV}^{-2} \text{ and } b_{el}^{\Psi(2S)} = 4.31 \pm 0.73 \text{ GeV}^{-2}$$

⁶ N. N. Nikolaev, B. G. Zakharov, Phys. Lett. B 332, 184, 1994

Light cone wave functions

Introduction

Cross
Section
Calculation

Results

Summary

The light cone wave functions of the mesons are written as:

$$\Psi_{h,\bar{h}}^{V,L}(r,z) = \sqrt{\frac{N_c}{4\pi}} \delta_{h,-\bar{h}} \frac{1}{M_V z(1-z)} \times [z(1-z)M_V^2 + \delta(m_f^2 - \nabla_r^2)] \phi_L(r,z)$$

where $\nabla_r^2 = (1/r)\partial_r + \partial_r^2$

$$\begin{aligned} \Psi_{h,\bar{h}}^{V,T(\gamma=\pm)}(r,z) = & \pm \sqrt{\frac{N_c}{4\pi}} \frac{\sqrt{2}}{z(1-z)} \{ ie^{\pm i\theta_r} [z\delta_{h\pm,\bar{h}\mp} - (1-z)\delta_{h\mp,\bar{h}\pm}] \partial_r \\ & + m_f \delta_{h\pm,\bar{h}\mp} \} \phi_T(r,z) \end{aligned}$$

$N_c \rightarrow$ color number.

$h, \bar{h} = \pm \frac{1}{2} \rightarrow$ quarks helicity.

Wave functions: Boosted Gaussian Wavefunction

$\Psi(1S)$ and $Y(1S)$:

$$\phi_{T,L}^{1S}(r, z) = \mathcal{N}_{T,L} Z(1-z) \exp \left\{ -\frac{m_f^2 \mathcal{R}_{1S}^2}{8z(1-z)} - \frac{2z(1-z)r^2}{\mathcal{R}_{1S}^2} + \frac{m_f^2 \mathcal{R}_{1S}^2}{2} \right\}$$

$\Psi(2S)$ and $Y(2S)$:

$$\phi_{T,L}^{2S}(r, z) = \mathcal{N}_{T,L} Z(1-z) \exp \left\{ -\frac{m_f^2 \mathcal{R}_{2S}^2}{8z(1-z)} - \frac{2z(1-z)r^2}{\mathcal{R}_{2S}^2} + \frac{m_f^2 \mathcal{R}_{2S}^2}{2} \right\} [1 + \alpha_{2S} g_{2S}(r, z)]$$

$$g_{2S}(r, z) = 2 - m_f^2 \mathcal{R}_{2S}^2 + \frac{m_f^2 \mathcal{R}_{2S}^2}{4z(1-z)} - \frac{4z(1-z)r^2}{\mathcal{R}_{2S}^2}$$

$\mathcal{N}_{T,L}, \mathcal{R}_{nS}^2, \alpha_{2S} \rightarrow$ parameters obtained from the wave functions orthogonality and normalization, relation to dilepton decay width ^{7, 8}

Meson	m_f (GeV)	\mathcal{N}_L	\mathcal{N}_T GeV	\mathcal{R}^2 (GeV ⁻²)	α_{2S}	M_V (GeV)	$\Gamma_{e^+e^-}^{\text{exp}}$ (KeV)	$\Gamma_{e^+e^-}$ (KeV)
J/ψ	1.4	0.57	0.57	2.45	0	3.097	5.55±0.14	5.54
$\psi(2S)$	1.4	0.67	0.67	3.72	-0.61	3.686	2.37±0.04	2.39
$Y(1S)$	4.2	-	0.481	0.567	0	9.46	1.34±0.018	1.34
$Y(2S)$	4.2	-	0.624	0.831	-0.555	10.023	0.612±0.011	0.611

⁷ N. Armesto and Amir H. Rezaeian, Phys. Rev. D90, 054003, 2014

⁸ B. E. Cox, J. R. Forshaw and R. Sandapen, JHEP06, 034, 2009

Dipole Cross Section - GBW

Introduction

Cross
Section
Calculation

Results

Summary

The GBW (Golec-Biernat and Wusthoff) parametrization is given by: ⁹

$$\sigma_{dip}(x, \vec{r}; \gamma) = \sigma_0 \left[1 - \exp\left(-\frac{r^2 Q_{sat}^2}{4}\right)^{\gamma_{eff}} \right]$$

$\gamma_{eff} = 1$, $m_c = 1.4 \text{ GeV}$

Saturation scale $\rightarrow Q_{sat}^2(x) = \left(\frac{x_0}{x}\right)^\lambda$

$GBW_{old}^9 \rightarrow Q_{sat}^2(x) = \left(\frac{x_0}{x}\right)^\lambda$ $\sigma_0 = 29.12$, $x_0 = 0.41 \times 10^{-4}$ and $\lambda = 0.277$

GBW_{new}^{10} (consider the effect of the gluon number fluctuations) $\rightarrow \sigma_0 = 31.85$,

$x_0 = 0.0546 \times 10^{-4}$ and $\lambda = 0.225$

⁹K. Golec-Biernat and M. Wusthoff, Phys. Rev. D 59, 014017, 1999

¹⁰M. Kozlov, A. Shoshi and W. Xiang, JHEP 0710, 020, 2007

Dipole cross section - CGC

Color Glass Condensate parametrization (CGC): ¹¹

$$\sigma_{q\bar{q}}^{CGC}(x, r) = \sigma_0 \times \begin{cases} N_0 \left(\frac{rQ_s}{2}\right)^{2(\gamma_s + (1/\kappa\lambda Y)\ln(2/rQ_s))}, & rQ_s \leq 2 \\ 1 - e^{-A\ln^2(BrQ_s)}, & rQ_s > 2 \end{cases}$$

$Q_s^{CGC} = (x_0/x)^{\lambda/2} \text{ GeV} \rightarrow$ saturation scale

$N_0 = 0.7, \kappa = 9.9 \rightarrow$ fixed to their LO BFKL values

R, x_0, λ and $\gamma_s \rightarrow$ free parameters of the fit (with $\sigma_0 = 2\pi R^2$)

$$A = \frac{-N_0\gamma_s^2}{(1-N_0)^2 \ln(1-N_0)}, \quad B = \frac{1}{2}(1-N_0)^{-(1-N_0)/N_0\gamma_s}$$

$CGC_{old} (m_c = 1.4 \text{ GeV})^{12} \rightarrow \sigma_0 = 27.33, x_0 = 0.1632 \times 10^{-4}, \lambda = 0.2197$ and $\gamma_s = 0.7376$

$CGC_{new} (m_c = 1.27 \text{ GeV})^{13} \rightarrow \sigma_0 = 21.85, x_0 = 0.6266 \times 10^{-4}, \lambda = 0.2319$ and $\gamma_s = 0.762$

¹¹E. Iancu, K. Itakura and S. Munier, Phys. Lett. B 590, 199, 2004

¹²G. Soyez, Phys. Lett. B 655,32, 2007

¹³A.H. Rezaeain and I. Schmidt, Phys. Rev. D 88, 074016, 2013

Color Glass Condensate parametrization (b-CGC):¹⁴

$$N_{q\bar{q}}^{bCGC}(x, r) = \begin{cases} N_0 \left(\frac{rQ_s}{2}\right)^{2(\gamma_s + (1/\kappa)\lambda Y)\ln(2/rQ_s)}, & rQ_s \leq 2 \\ 1 - e^{-A\ln^2(BrQ_s)}, & rQ_s > 2 \end{cases}$$

$$Q_s^{bCGC} = (x_0/x)^{\lambda/2} \left[\exp\left(-\frac{b^2}{2B_{CGC}}\right) \right]^{1/2\gamma_s} \text{ GeV} \rightarrow \text{saturation scale}$$

$$B_{CGC} = 7.5 \text{ GeV}^{-2}$$

$\gamma_s = 0.46$ and $\kappa = 9.9 \rightarrow$ fixed to its LO BFKL value

$x_0, \lambda \rightarrow$ free parameters of the fit

$$A = \frac{-N_0\gamma_s^2}{(1-N_0)^2 \ln(1-N_0)}, \quad B = \frac{1}{2}(1-N_0)^{-(1-N_0)/N_0\gamma_s}$$

$b\text{-CGC}_{old}^{14} \rightarrow x_0 = 0.0184 \times 10^{-4}, \lambda = 0.119$ and $\gamma_s = 0.46$

¹⁴ G. Watt and H. Kowalski, Phys. Rev. D 78, 014016, 2008

$\Psi(1S)$ and $\Psi(2S)$ cross check

Integrated cross section:

Table: Total cross section in the rapidity region $2.0 < \eta < 4.5$ (in units of pb) for photoproduction of the $\psi(1S, 2S)$ (**corrected for acceptance**) states in pp collisions at $\sqrt{s} = 7$ TeV compared to the LHCb data ¹⁵.

$\sigma_{pp \rightarrow J/\psi \rightarrow \mu^+ \mu^-}$	<i>GBW</i>	<i>CGC^{old}</i>	<i>CGC^{new}</i>	<i>BCGC^{old}</i>	<i>GBW^{ksx}</i>	LHCb measure
$\psi(1s)$	277.60	213.69	199.58	154.57	170.81	291 ± 20.24
$\psi(2s)$	8.40	5.94	5.98	4.13	4.39	6.5 ± 0.98

Cross section ratio (with BG wave function):

$$[\psi(2S)/\psi(1S)]_{2 < y < 4.5} = 0.028 \pm 0.02$$

$$\text{LHCb: } [\psi(2S)/\psi(1S)](2.0 < \eta_\mu < 4.5) = 0.022$$

¹⁵LHCb Collaboration, J. Phys. G 41, 055002, 2014.

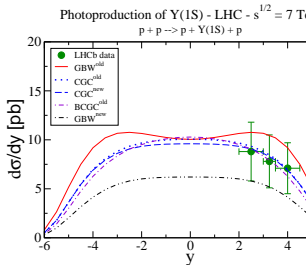
Y(1S) rapidity distribution in pp collisions at 7 TeV

Introduction

Cross
Section
Calculation

Results

Summary



- Predictions to rapidity distribution at LHC (7 TeV) for pp collisions ^a;

- The models GBW, CGC and b-CGC were considered for the dipole cross section ($m_b = 4.5$ GeV);

$$B_V(W_{\gamma p}) = b_{el}^V + 2\alpha' \log\left(\frac{W_{\gamma p}}{W_0}\right)^2$$

$$\alpha' = 0.164 \text{ GeV}^{-2}$$

$$W_0 = 95 \text{ GeV}$$

$$b_{el}^\Upsilon = 3.68 \text{ GeV}^{-2}$$

^aLHCb Coll., JHEP 1509, 084 (2015)

Figure: The rapidity distribution of Y(1S) photoproduction at $\sqrt{s} = 7$ TeV

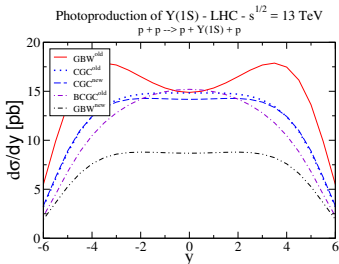
$Y(1S)$ and $Y(2S)$ rapidity distribution in pp collisions at 13 TeV

Introduction

Cross
Section
Calculation

Results

Summary



- Predictions to rapidity distribution at LHC (13 TeV), for pp collisions;
- The models GBW and CGC were considered for the dipole cross section;

Figure: The rapidity distribution of $Y(1S)$ and photoproduction at $\sqrt{s} = 13 \text{ TeV}$

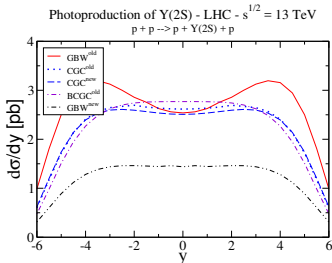
$Y(1S)$ and $Y(2S)$ rapidity distribution in pp collisions at 13 TeV

Introduction

Cross
Section
Calculation

Results

Summary



- Predictions to rapidity distribution at LHC (13 TeV), for pp collisions;
- The models GBW and CGC were considered for the dipole cross section;

Figure: The rapidity distribution of $Y(2S)$ and photoproduction at $\sqrt{s} = 13 \text{ TeV}$

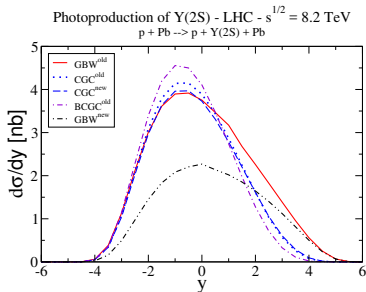
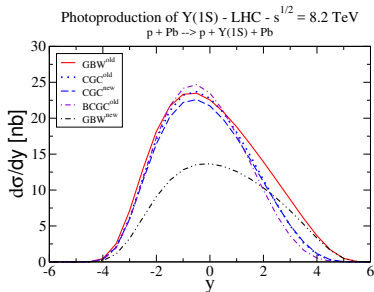
Prediction for pA collisions

Introduction

Cross
Section
Calculation

Results

Summary



- Predictions to rapidity distribution at LHC (8.2 TeV) for pA collisions.

$Y(1S)$, $Y(2S)$ production in AA collisions

Introduction

Cross
Section
Calculation

Results

Summary

Coherent process:



\Rightarrow nuclei remain intact.

Incoherent process:



\Rightarrow involves modification of one of the participating nuclei.

Coherent $Y(1S)$, $Y(2S)$ production in AA collisions

Introduction

Cross
Section
Calculation

Results

Summary

Incoherent cross section: ¹⁶

$$\sigma^{coh}(\gamma A \rightarrow VA) = \int d^2b \left\{ \left| \int d^2r \int dz \Psi_V^*(r, z) \right. \right. \\ \left. \left. \times \left(1 - \exp \left[-\frac{1}{2} \sigma_{dip}(x, r) T_A(b) \right] \right) \Psi_{\gamma^*}(r, z, Q^2) \right|^2 \right\}$$

$\sigma_{dip} \rightarrow$ dipole cross section.

$\Psi_V \rightarrow$ vector meson wave function.

$\Psi_{\gamma} \rightarrow$ photon wave function.

$$T_A(b) = \int dz \rho_A(b, z)$$

$\rho_A(b, z) \rightarrow$ nuclear thickness function.

$b \rightarrow$ impact parameter.

¹⁶B. Z. Kopeliovich and B. G. Zakharov, Phys. Rev. D 44, 3466, 1991

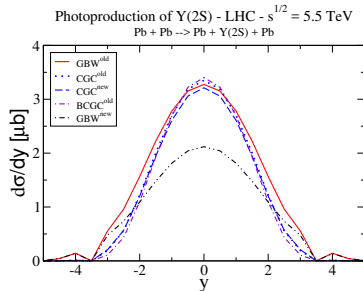
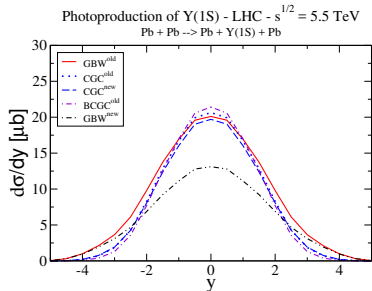
Rapidity distribution in Pb-Pb collisions for $\Upsilon(1S)$, $\Upsilon(2S)$

Introduction

Cross
Section
Calculation

Results

Summary



- Predictions to rapidity distribution at LHC (5.5 TeV) for AA collisions.

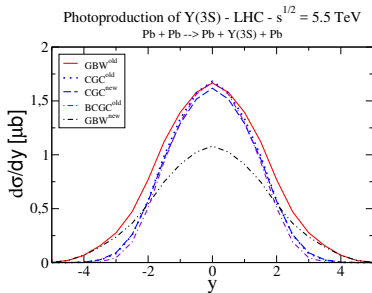
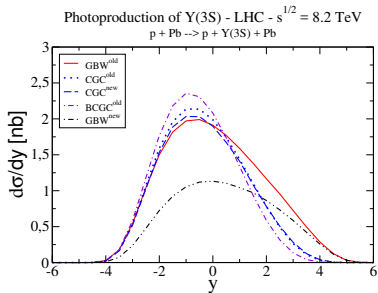
$\Upsilon(3S)$ rapidity distribution in pPb and PbPb collisions

Introduction

Cross
Section
Calculation

Results

Summary



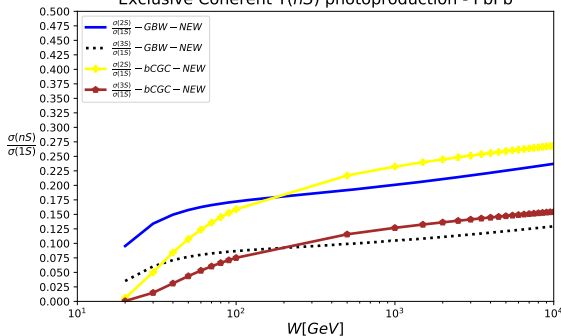
- Predictions for rapidity distribution of $\Upsilon(3S)$ state in for pA and AA collisions.

Relative contribution of radial states in PbPb

Coherent cross section ratios (for distinct dipole models): 17

$$\frac{\sigma(nS)}{\sigma(1S)} = \frac{\sigma(\gamma A \rightarrow \Upsilon(nS)A)}{\sigma(\gamma A \rightarrow \Upsilon(1S)A)}$$

Exclusive Coherent $\Upsilon(nS)$ photoproduction - PbPb



17 Gay Ducati, Kopp, MVTM, Phys. Rev. D 96, 054001, 2017

Incoherent $Y(1S)$, $Y(2S)$ production in AA collisions

Introduction

Cross
Section
Calculation

Results

Summary

Incoherent cross section: ¹⁸

$$\sigma^{inc}(\gamma A \rightarrow VA^*) = \int d^2b \frac{T_A(b)}{16\pi B_V} \left\{ \left| \int d^2r \int dz \Psi_V^*(r, z) \right. \right. \\ \left. \left. \times \left[\sigma_{dip}(x, r) \exp\left(-\frac{1}{2}\sigma_{dip}(x, r)T_A(b)\right) \right] \Psi_\gamma(r, z, Q^2) \right|^2 \right\}$$

$\sigma_{dip} \rightarrow$ dipole cross section.

$\Psi_V \rightarrow$ vector meson wave function.

$\Psi_\gamma \rightarrow$ photon wave function.

$$T_A(b) = \int dz \rho_A(b, z)$$

$\rho_A(b, z) \rightarrow$ nuclear thickness function.

$b \rightarrow$ impact parameter.

¹⁸B. Z. Kopeliovich and B. G. Zakharov, Phys. Rev. D 44, 3466, 1991

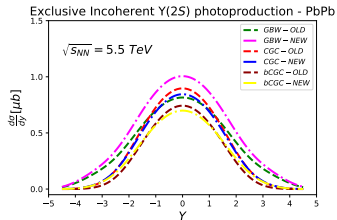
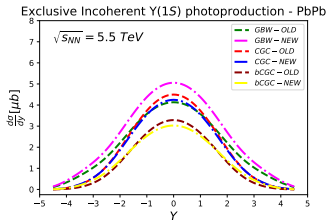
Rapidity distribution in incoherent Pb-Pb collisions for $\Upsilon(1S)$, $\Upsilon(2S)$

Introduction

Cross
Section
Calculation

Results

Summary



- Predictions to rapidity distribution at LHC (5.5 TeV) for PbPb collisions.

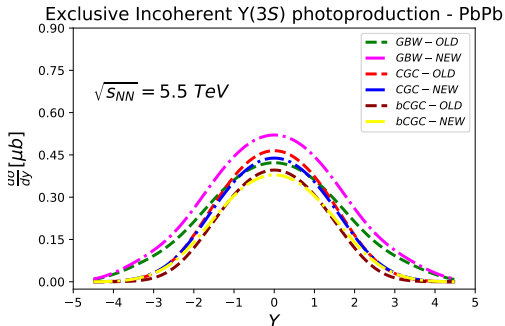
$\Upsilon(3S)$ rapidity distribution in incoherent PbPb collisions

Introduction

Cross
Section
Calculation

Results

Summary



- Predictions for rapidity distribution of $\Upsilon(3S)$ state in incoherent AA collisions.

Summary

Introduction

Cross
Section
Calculation

Results

Summary

pp:

- The rapidity distributions of mesons $\Psi(1S)$, $\Psi(2S)$, $\Upsilon(1S)$ and $\Upsilon(2S)/\Upsilon(3S)$ production were calculated in pp collisions using the dipole formalism. Focus on the Upsilon states.
- The predictions for $\Psi(1S)$ and $\Psi(2S)$ rapidity distributions and integrated cross sections are consistent with LHCb data.
- The results for $\Upsilon(1S)$ are consistent with LHCb data and predictions to higher energies have been done. Some results for pA case were presented.

PbPb:

- The coherent production of mesons $\Upsilon(1S)$ and $\Upsilon(2S, 3S)$ has been calculated in Pb-Pb collisions using the dipole formalism (including relative contributions).
- Results for incoherent $\Upsilon(nS)$ production in $PbPb$ were presented for sake of completeness.



Introduction

Cross
Section
Calculation

Results

Summary

Thank You!